Study of All-Optical Wavelength Conversion and Regeneration Subsystems for use in Wavelength Division Multiplexing (WDM) Telecommunication Networks.

Hercules Simos *

National and Kapodistrian University of Athens
Department of Informatics and Telecommunications

simos@di.uoa.gr

Abstract. In this thesis, we study all-optical processing techniques based on non-linear semiconductor optical amplifiers for the functionalities of second and third generation optical networks. In particular, devices for all-optical wavelength conversion with regenerative properties have been investigated. The configurations under investigation are based on the non-linear four-wave mixing process which occurs when fields with proper spectral and power arrangement are coupled into the active medium. The performance characteristics of the devices are determined by the properties of the optical amplifier, as well as by the operating conditions like the gain of the optical amplifier, the power levels and the frequency detuning of the pump and the information signal.

Keywords: All-optical wavelength conversion, four wave mixing, regeneration, semiconductor optical amplifier, amplified spontaneous emission noise.

1 Introduction

All-optical wavelength conversion is considered as a key function for the future WDM lightwave systems. Wavelength conversion addresses a number of key issues in WDM networks including transparency, interoperability, and network capacity. Wavelength conversion may be the first obstacle in realizing a transparent WDM network. High bit rate and efficient conversion has been demonstrated using techniques like cross-gain modulation (XGM), cross phase modulation (XPM) and four wave mixing (FWM) in a variety of passive or active media [1]. FWM in traveling wave semiconductor optical amplifiers (TW-SOAs) is probably the most favored and studied technique for λ-conversion, since it offers transparency to the modulation format and to the applied data rate up to tens of Gbps [1].

On the other hand, in high bit rate optical communication systems and networks, data signals suffer from degradation during their propagation, due to noise, pulse

* Dissertation Advisor: Dimitris Syvridis, Professor

distortion and crosstalk. The accumulation of amplified spontaneous emission (ASE) noise generated by amplifiers degrades the signal to noise ratio (SNR). Chromatic dispersion affects the pulse shape, while different types of crosstalk due to the propagation through optical cross connects, wavelength converters and filters, degrade the signal quality. All-optical regenerators are critical components for the restoration of these signal impairments, avoiding the optoelectronic conversion limitations. Regeneration can be either 2R for signal reshaping, or 3R for both signal reshaping and retiming. Several regenerators have been proposed so far, based on XPM, cross-gain modulation XGM in passive or active media. Although the four-wave mixing process is (FWM) is exhaustively investigated for λ-conversion applications, only recently, FWM in DSF has been employed as a 2R all-optical regenerator [2], [3].

In this thesis, we study all-optical processing techniques based on non-linear semiconductor optical amplifiers for the functionalities of second and third generation optical networks. In particular, devices for all-optical wavelength conversion with regenerative properties, based on FWM in a SOA, have been investigated in detail. In the first part of this thesis, the noise properties of the converted signal generated by the four-wave mixing based wavelength conversion process were investigated. The investigation of the noise characteristics was carried out by a theoretical analysis and the corresponding experimental confirmation, including the separate study of noise induced by the four wave mixing process itself and the amplified spontaneous emission noise from the amplifier. The study of the noise properties at the new wavelength was performed for the intensity as well as the phase noise of the converted signal. The useful conclusions from this study were used for the investigation of the regenerative properties of the mixing process.

The second part of this thesis starts with the experimental investigation and the confirmation of the regenerative properties of the four wave mixing process in a semiconductor optical amplifier. The regeneration and simultaneous wavelength conversion of 2.5 Gbps optical signals is experimentally demonstrated. Furthermore, the second part includes the design and optimization by numerical simulation of a wavelength conversion system with regenerative properties, for use in nodes of wavelength division multiplexing optical networks. In this thesis, an alternative configuration for the pump and data signal is proposed for the first time, in order to obtain non-linear response from the optical amplifier. Based on this approach the new signal exhibits improved noise characteristics and lower bit error rate. The numerical investigation showed successful regenerative operation at 40 Gbps.

2 Numerical modeling of FWM in SOAs

The FWM process in a SOA can be generally described as follows. Pump (A_1) and signal (A_2) waves at optical frequencies ω_1 and ω_2 respectively, with the same state of polarization, are injected into the SOA from the same facet. The beating of the two co-propagating input waves inside the SOA generates refractive index and gain gratings at the frequency $\Omega = \omega_2 - \omega_1$. The input waves are scattered by these gratings which in turn leads to the creation of product waves, the conjugate (A_3) and the

satellite (A_4) at optical frequencies ω_3 and ω_4 respectively, with $\omega_3 = \omega_1 - \Omega = 2\omega_1 - \omega_2$ and $\omega_4 = \omega_2 + \Omega = 2\omega_2 - \omega_1$. The numerical analysis is based on the position dependent gain rate equation and the field propagation equations. The propagation and the nonlinear interaction between the input waves and the FWM products are described by the coupled - mode equations. The expression for the first FWM signal is given below [4]:

$$\frac{\partial A_3}{\partial z} = \frac{1}{2}[g(1 - i\alpha_{CDP}) - a_{loss}]A_3 - \frac{1}{2}\left(\eta_{3,1}|A_1|^2 + \eta_{3,2}|A_2|^2 + \eta_{3,4}|A_4|^2\right)A_3 - \frac{1}{2}(\eta_{1,4} + \eta_{2,4})A_1 A_2 A_4^* - \frac{1}{2}\eta_{1,2}A_1^2 A_2^* + A_{SE,3} \quad (1)$$

The variation of the time dependent gain $g = g(z, t)$, for a subsection is given by [4]:

$$\frac{\partial g}{\partial t} = \frac{g_s - g}{\tau_s} - g \cdot \frac{P_{tot}}{P_{sat}\tau_s} \quad (2)$$

$A_i = A_i(z, t)$, $i = 1, 2, 3, 4$, is the slowly varying envelope of the fields; $A_{SE,i} = A_{SE,i}(z,t)$, represents the spontaneous emission noise generated and added to the waves in each subsection; it is modeled as a white Gaussian distributed process [4]; The coefficients $\eta_{i,j}$, $i, j = 1, 2, 3, 4$, $i \neq j$, represent the non-linear interactions among the mixing waves, which they are related to the inter-band and intra-band carrier dynamics: the carrier density pulsations (CDP), the carrier heating (CH) and the spectral hole burning (SHB). The expression for each mechanism, as well as all other parameters can be found in [4], [5]. The four output fields $A_i = A_i(z = L, t)$, $i = 1, 2, 3, 4$, are calculated by numerically integrating the equations (1) and (2) over the SOA length. Integration is accomplished by sampling the length of the SOA at subsections of length dz and the time-dependent fields at samples of duration dt. The simulations are carried out employing either continuous waves (CW) or Non Return to Zero (NRZ) pulsed inputs.

3 Noise properties of FWM in a SOA

The major drawbacks of the FWM process in SOAs, are the efficiency degradation at high detuning values and the optical signal-to-noise ratio (OSNR) degradation due to the amplified spontaneous emission (ASE). In general the spontaneous emission perturbs both the amplitude and phase of the converted signal, resulting to its intensity and phase noise degradation.

3.1 RIN performance of wavelength converters based on FWM in SOAs

The relative intensity noise (RIN) properties of the FWM converted signal have not been investigated up to now, neither theoretically nor experimentally. Such an

investigation is necessary since RIN affects the performance of lightwave systems using intensity modulation. In this section the numerical and experimental study on the RIN performance of the FWM in SOAs is presented. The influence of the power as well as the intensity noise properties of the input signals, was investigated. Although in most cases a degradation of the converted signal is observed, it will be shown that improvement in the RIN performance is possible under certain operating conditions [5]. This property reveals the regenerative capability of the FWM process.

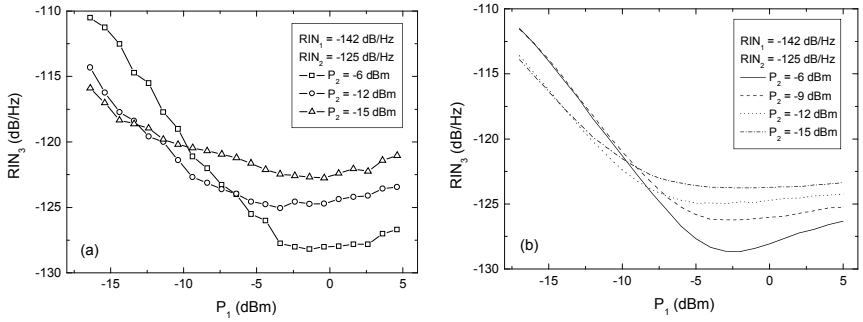

Fig. 1. RIN of the wavelength converted signal against input pump power with $RIN_1 = RIN_2 =$ -142 dB/Hz: (a) experimental and (b) numerical results.

The intensity noise of the converted signal against input power is shown in fig. 1. Figure 2 depicts the dependence of the output signal RIN (RIN_3) on the input pump power (P_1) for different levels of the input power of the signal (P_2). Figure 1a corresponds to experimental data and figure 1b to calculated results. In both cases the RIN of the input signals was RIN_1 = -142 dB/Hz and RIN_2 = -125 dB/Hz. The dependence of the output RIN on the pump power (P_1) is not monotonous, but it exhibits a saturation regime at high pump power levels. In addition, the output RIN depends inversely proportional on the input signal power (P_2), at high levels of P_1. The latter does not hold for low power levels of A_2 (P_2). In this case, the roles of the two input waves change as A_2 becomes the pump and A_1 the signal. The explanation for the behavior of fig. 1 can be given through the power transfer functions of the FWM process. As P_1 increases, the conversion efficiency gradually saturates reaching the regime where further increase of P_1 results in constant or even decreasing P_3. This regime appears at higher P_1 values as P_2 increases. At the same time the SOA gain has reached already the saturation, resulting in a more or less constant level of ASE noise. This means that for the P_1 range where the conversion efficiency is not saturated, while the ASE noise is saturated, the output RIN decreases with P_1, as observed in fig. 1. Further increase of P_1, results in decrease of the converted signal power and therefore increase of the RIN_3, in agreement with the experimental and numerical findings of fig. 1.

An interesting finding from fig. 1, which could lead to useful conclusions from the application point of view, is related to the fact that the output RIN_3 is lower relative to the input signal noise RIN_2. This occurs in the saturation regime (high pump power levels) when the signal power is also high (e.g. in fig. 1, curves corresponding to P_2 = -6 dBm, P_2 = -9 dBm). In order to clarify the physical mechanism behind this

behavior, calculations of RIN_3 against P_1 have been carried out, assuming a noise-free SOA. It was found that when the input noise is low (RIN_1 = RIN_2 = -142 dB/Hz) the output noise RIN_3 in the saturation regime is close to the input RIN_2. In the case where the input signal noise is higher (RIN_1 = -142 dB/Hz, RIN_2 = -125 dB/Hz), RIN_3 is reduced with respect to the input RIN_2. For the pump power level where the process is unsaturated, the combination of the low output power P_3 with the high noise from the signal, leads to output RIN_3 levels close to the high input value RIN_2.

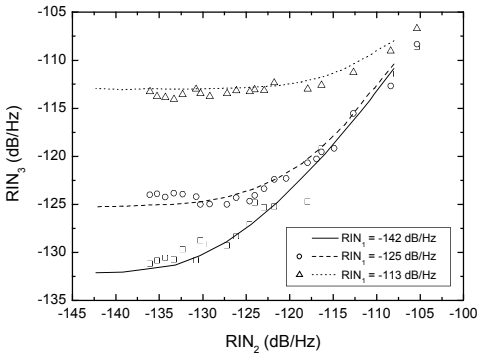

Fig. 2. Output noise RIN_3 versus input signal noise RIN_2, for different levels of the input pump noise RIN_1. Lines correspond to numerical calculations and symbols represent experimental data. P_1 = 0 dBm, P_2 = -6 dBm

In order to confirm the input noise influence, the dependence of RIN_3 on RIN_2 has been investigated both numerically and experimentally (fig. 2), for different levels of RIN_1. The power levels of P_1 and P_2 have been properly chosen in order to ensure highly efficient conversion. A general observation that can be made is that the upper limit of RIN_3 is set by the signal noise (RIN_2), while the lower limit is set by the pump noise (RIN_1), except of the case of very low RIN_1 (-142 dB/Hz) where the lower limit is set by the ASE noise. The limit on the lower values is no longer set by the pump noise, when the input value of RIN_1 is very low.

It is obvious from the above discussion, that the overall RIN performance of the converter is a combination of two discrete processes. The first is the ASE noise and its dependence on the input power. The second is the transfer of the intensity noise from the input waves, to the output through the FWM process. ASE dominates in the low pump power regime, where the FWM efficiency is poor, whereas at the saturation regime, RIN carried by the input signal predominates over ASE.

3.2 Phase noise performance of wavelength converters based on FWM in SOAs

The result of this part was a detailed theoretical and experimental study of the phase noise characteristics of FWM in a SOA based wavelength converters. The theoretical study for the spectral linewidth of the conjugate, the new four-wave mixing component used for conversion, predicted that the new wave has a spectral

linewidth strongly dependent on the pump linewidth (x4) plus the probe linewidth. This effect was confirmed by experimental results for several operating conditions (different amplifiers, input linewidth). The results showed that the linewidth of the converted signal is independent of the amplified spontaneous emission noise induced from the amplifier, and that the linewidth enhancement observed, is caused by the non linear dynamics of the four wave mixing process. The numerical investigation confirmed the analytical theory for in high pumping conditions, however low pump power induces high levels of phase noise to the conjugate due to strong influence of ASE noise.

3 Experimental investigation of the regenerative properties of FWM in a SOA

In this part, the possibility to achieve extinction ratio (ER) enhancement and noise suppression in SOA based FWM λ-converters, is investigated for the first time in detail, assuming NRZ data format carried by one of the optical inputs according to the typical wavelength conversion operating scheme. We show that in most cases the SOA saturation dominates resulting even in ER degradation of the output relative to the input. Nevertheless there is an operating regime where significant ER enhancement can be achieved together with noise suppression while the obtained output remains NRZ modulated. The experimental setup for the measurements under dynamic operation is shown in fig. 3.

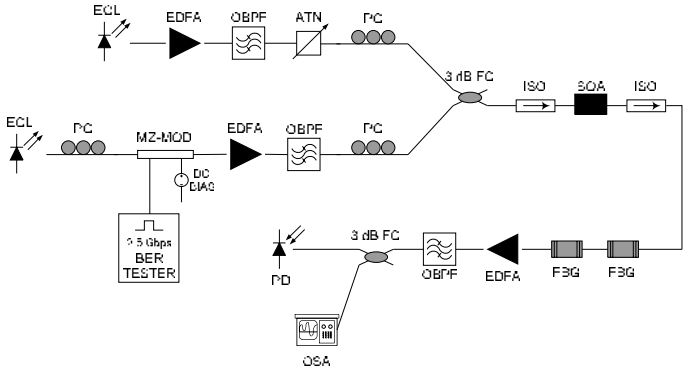

Fig. 3 The experimental setup used for the dynamic measurements of the wavelength conversion based on FWM in a SOA. EDFA: erbium-doped fiber amplifier, BPF: band-pass filter, PC: polarization controller, MOD: modulator, SOA: semiconductor optical amplifier, OI: optical isolator, FBG: fiber Bragg grating.

In order to characterize the regenerative properties of the FWM process, the static transfer function of the process was experimentally determined by measuring the output power of the conjugate product as a function of the pump wave input optical power while keeping the signal wave optical power, at a constant value. The results, for three different optical power values of the signal (16 μW, 35 μW and 50 μW) are

shown in fig. 4a. The results show a well understood behavior discussed already in the past [6]. The conjugate optical power assuming operation in the unsaturated regime, is given by $P_3 = G_1^2 G_2 P_1^2 P_2 R(\Omega)$ where P_1 and P_2 are the pump and signal optical power respectively, G_1, G_2 are the corresponding small signal gain and $R(\Omega)$ depends on the detuning between signal and pump. Only at small signal conditions and with totally unsaturated SOA the gain remains constant and therefore the optical power of the conjugate depends on the square of the pump power, resulting in extinction ratio improvement of the FWM product. Such conditions are practically infeasible as it shown in fig. 4a. Even for very low signal power of 16 μW and accordingly low pump power levels, the conjugate power increases for a while as the pump power reaches to a value of approximately 80 μW. Further increase of the pump results in decreasing the conjugate power due to the gain saturation of the SOA.

For the conditions of the transfer function corresponding to $P_1 = 50$ μW, dynamic measurements were carried out; the corresponding results (fig. 4b) show enhancement of the output extinction ratio of 2-3 dB. Bit error rate measurements showed a 1-3 dB improvement (negative sensitivity penalty) of the regenerated output versus the input signal and for BER values in the range from 10^{-11} to 10^{-7} [7]. Fig. 4b (inset) shows eye diagrams of the signal at the input (lower) and the regenerated output (upper).

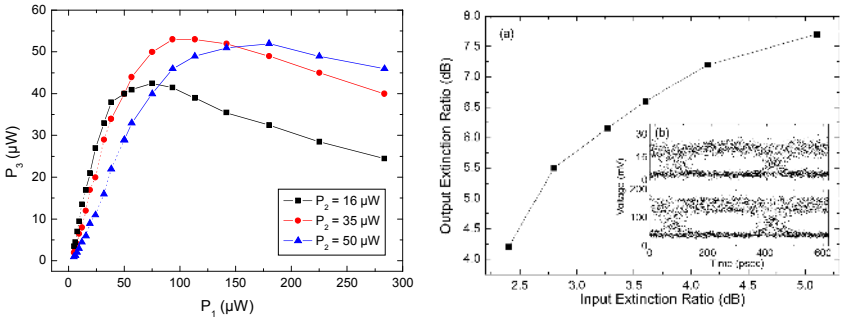

Fig. 4 (a) Experimental transfer functions of FWM in a SOA (b) experimental dynamic measurements of the output extinction ratio versus the input ER.

4 Design and numerical evaluation of a wavelength converter with 2R regenerative properties based on FWM in a SOA

Up to now, none of the conventional FWM configurations have exhibited regenerative properties. The experimental investigation of the previous section showed that if the data stream is applied on the pump wave instead of the signal, and under certain conditions for the power levels of the modulated wave relative to the CW one, regenerative characteristics appear at the λ-converted wave. However, the nature of the FWM based regeneration process, which is related to the SOA's gain saturation, sets an upper limit at the operation speed of the whole process due to the limited response of the SOA's carrier dynamics. Major objectives of the present

section is to investigate the above speed limitations and to identify the optimum SOA's structural characteristics as well as FWM operational conditions at which regenerative behavior is expected. In order to increase the maximum achievable bit rate for this type of regenerator, a fiber Bragg grating (FBG) is employed at the output of the SOA, to act as an optical discriminator increasing this way significantly the upper limit of the bit rate operation of the regenerator. The study is structured as follows: the numerical model is solved numerically for the case of CW inputs, in order to calculate a set of static transfer functions of the regenerator corresponding to different FWM operating conditions. Using these static transfer functions, the operating conditions which correspond to the best regenerative performance, are identified. Based on the optimized operating conditions, the above FWM model is solved in the time domain with NRZ modulated input data up to 40 Gbps, and the corresponding output ER and Q-factor are calculated.

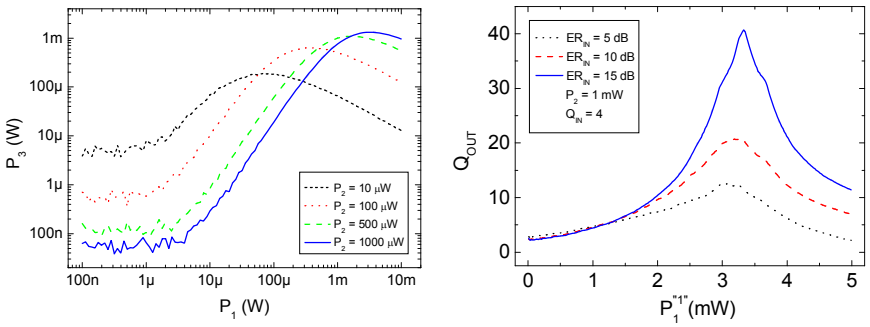

(a) (b)

Fig. 5 (a) Static $P_3(P_1)$ transfer functions of the FWM process in a SOA. (b) The expected Q-factor at the output, calculated using the transfer function with P_2 = 1000 μW shown in (a).

4.1 Static results

The optical power P_3, of the product A_3 is plotted against the power P_1 of the input wave A_1 (fig. 5a), for different power levels P_2 of the input wave A_2, according to the FWM configuration mentioned above. Obviously from the group of curves of figure 5a, the increase of P_2 results in a much more satisfactory non-linear transfer function like the one of the ideal regenerator. The $P_3(P_1)$ behavior has been observed and discussed in the past [6]. Using the transfer function corresponding to P_2 = 1000 μW of figure 5a, we calculated the output Q-factor and extinction (ER) for a constant input Q factor of 4 and for different input ER values. The output Q-factor is plotted in fig. 5b. It is obvious that, the best performance in terms of Q-factor is achieved when the input power level of A_1 is in the saturation regime of the transfer function. On the contrary, maximum ER enhancement is achieved at lower input power levels, corresponding to the linear regime of the transfer function.

Similar calculations have been performed to study the wavelength detuning between the input signals and the SOA length influence to the regenerator's static

performance. It is shown [4] that low values of wavelength detuning and long SOAs device are preferable for our application where high conversion efficiency is critical.

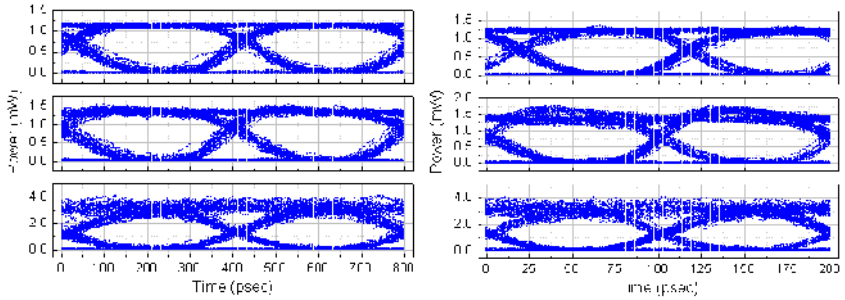

Fig. 6. Calculated eye diagrams at the input, at the SOA output and at the FBG output (from bottom to top) for operation at (a) 2.5 Gbps and (b) 10 Gbps.

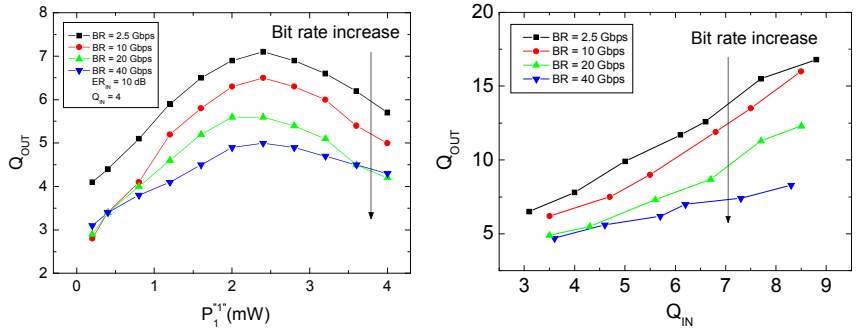

Fig. 7. Calculated Q-factor at the input, as a function (a) of the input power of the logic symbol "1" and (b) of the input Q-factor, for different bit rates.

4.2 Dynamic results

As mentioned earlier, the dynamic behavior of the FWM based regenerator is expected to be much different from the static one. This is because, at the dynamic operation of the system, several speed limitations are imposed by the SOA carrier dynamics, which do not appear at a typical FWM scheme. Due to the strong variation of P_1 and the fact that a part of the regeneration process is based on the SOA gain saturation, it can be easily shown both theoretically and experimentally, that the regenerator's performance at high data rates is limited by the carrier dynamics of the SOA. Typical eye diagrams at 2.5 and at 10 Gbps are shown at figure 6a and 6b, respectively. In the case of 2.5 Gbps very satisfactory results are obtained in both ER improvement and noise suppression even without the use of the grating filter. In the case of 10 Gbps, the noise suppression achieved by the FWM process is degraded by the pattern dependent response of the SOA (fig. 6b, middle), and finally restored by the FBG (fig. 6c, up). The FBG acts as a differentiator and restores the integration action of the SOA. Therefore, the overall regeneration performance at high bit rates is

a result of the combined action of the FWM originated noise suppression and the SOA speed enhancement through the FBG filter.

In fig. 7a we have plotted the output Q-factor as a function of the power level of the pump wave A_1, and in 7b the output Q versus the input Q, at several bit rates. The optimum performance for all rates occurs when the power of logic "1" is located at the saturated regime, we have maximum noise suppression for "1" power levels. Moving toward higher bit rates (10, 20, and 40 Gbps), a degradation mainly to the Q-factor performance, is observed. The degradation of the regeneration process is mainly caused by the speed limitations of the SOAs carrier dynamics as aforementioned. At 10 Gbps, there are remarkable regenerative characteristics. While at 20 Gbps, the performance is further decreased, and finally, at 40 Gbps, the regenerative behavior of the system is observed only at high values of the input ER. Finally the output Q shows linear dependence on the input Q for all rates.

5 Conclusions

Detailed investigation of the possibility to achieve all optical 2R regeneration using FWM in SOAs has been carried out. The alternative configuration of FWM proposed in this thesis is mainly determined by the operating conditions, mainly by the adjustment of the input power levels of the modulated signal. The FWM static transfer functions approximate the step-like characteristic of an ideal regenerator. The noise properties of the converted signal were investigated. The useful conclusions from this study were used for the investigation of the regenerative properties of FWM process. The expected regeneration properties are confirmed experimentally under static and dynamic operation at 2.5 Gbps optical signals. Furthermore, the design and optimization by numerical simulation of a wavelength conversion system with regenerative properties showed successful regenerative operation up to 40 Gbps.

References

1. S. J. B. Yoo, "Wavelength conversion technologies for WDM network applications," J. Lightw. Technol., vol. 14, pp. 955–966 (1996)
2. E. Ciaramella, S. Trillo, "All-Optical Signal Reshaping via Four-Wave Mixing in Optical Fibers", IEEE Photon. Technol. Lett., vol. 12, pp. 849-851 (2000)
3. A. Bogris and D. Syvridis, "Regenerative properties of a pump-modulated four wave mixing scheme in dispersion shifted fibers", J. Lightw. Technol., vol. 21, pp. 1892-1902, (2003)
4. H. Simos, A. Bogris, and D. Syvridis, "Investigation of a 2R all-optical regenerator based on four-wave mixing in a semiconductor optical amplifier", J. Lightw. Technol., vol. 22, pp. 595–604 (2004)
5. H. Simos, I. Stamataki and D. Syvridis, "Relative intensity noise performance of wavelength converters based on four-wave mixing in semiconductor optical amplifiers", IEEE J. of Quantum Electron., vol. 43, pp. 370-377, (2007).
6. A. D'Ottavi, E. Iannone, A. Mecozzi, S. Scotti, P. Spano, R. Dall'Ara, J. Eckner, G. Guekos, "Efficiency and noise performance of wavelength converters based on FWM in semiconductor optical amplifiers", IEEE Photon. Technol. Lett., vol. 17, pp. 357-359 (1995)

7. H. Simos, A. Argyris, D. Kanakidis, E. Roditi, A. Ikiades, and D. Syvridis, “Regenerative properties of wavelength converters based on FWM in a semiconductor optical amplifier”, IEEE Photon. Technol. Lett., vol. 15, pages 566–568 (2003)